Vibration-Rotation Spectra, the Coriolis Coupling Constants and the Intramolecular Force Field of Symmetric Top Molecules. I. The E-type Fundamental Bands of Methyl and Methyl-d_3 Halides

By Yonezo MORINO and Junko NAKAMURA*

(Received August 10, 1964)

It is a current problem in the determination of the intramolecular force field that a set of force constants must be chosen in such a way that they may reproduce not only the vibrational frequencies but also all the available observables that are related to the force field. Many attempts have been made to determine the intramolecular force field by using observed data of the Coriolis coupling constants as additional observables, especially in the case of molecules with methyl groups.[1a,b] As for the methyl halide molecules, however, the reported values of the Coriolis coupling constants are considered to be neither complete nor precise enough for the present purpose.[2-16] A systematic reinvestigation of infrared spectra has, therefore, been undertaken in the present study for the six species of methyl halides (CH_3Cl, CD_3Cl, CH_3Br, CD_3Br, CH_3I and CD_3I). The present report is limited to the experimental results on the E-type fundamental bands. The results of the force-field calculation and the analyses of overtones and combination bands will be reported in the succeeding papers of this series.

Eighteen vibration-rotation spectra, ν_4, ν_5 and ν_6 of six molecules, were resolved in the present study, and some of the previous subband assignments were revised. Analyses of the vibration-rotation bands gave the Coriolis coupling constants, the rotational constants and the frequencies of the vibrational band origins. A few bands show peculiar features which indicate the presence of perturbations, which probably influence some of the resulting data. Nevertheless, the "parallel nature" observed for the molecules investigated suggests the certainty of the present results. The assumption of the "parallel nature" was also extensively used to estimate the rotational correction terms through which the r_0 and r_e structures were estimated.

Experimental

Preparation of Samples. — All the compounds except CH_3I were prepared by the direct halogenation of CH_3OH or CD_3OH. Commercial CH_3I was used after low-temperature distillation in vacuo through a U-tube packed with grained potassium hydroxide and calcium chloride. CD_3OH was synthesized by the method described by Edgell and Parts[17] with some modifications; Ethylene carbonate, prepared from sodium ethylene glycolate and ethyl chloroformate, was reduced with $LiAlD_4$ to a complex compound which was then decomposed to CD_3OH with monobutylcarbitol in diethylcarbitol. About 1.6 g. of CD_3OH was obtained by this method starting from 2 g. of $LiAlD_4$.

CH_3Cl (CD_3Cl) and CH_3Br (CD_3Br) were prepared from alcohols by halogenation with phosphorus trichloride and phosphorus tribromide respectively. Sample gases were purified with potassium hydroxide, concentrated sulfuric acid and phosphorus pentoxide. CH_3OH was iodized to CD_3I by means of hydroiodic acid after the method of Cox, Tunner and Warner.[18]

The purities of the starting and the intermediate reagents as well as of the last products were examined by their physical constants, elemental analyses and spectroscopic analyses. The percentage of deuterium in CD_3X samples was not tested, but the existence of serious impurities (CH_2DX, CHD_2X,

---

* Present address: The Institute of Physical and Chemical Research, Komagome, Bunkyo-ku, Tokyo

1) a) I. Nakagawa and T. Shimanouchi, *J. Chem. Soc. Japan, Pure Chem. Sec.* (*Nippon Kagaku Zasshi*), **80**, 128 (1959); b) I. M. Mills, *Spectrochim. Acta*, **16**, 35 (1960); **18**, 1073 (1962); **19**, 1967 (1963).

2) W. H. Bennett and C. F. Meyer, *Phys. Rev.*, **32**, 888 (1928).

3) A. H. Nielsen and E. F. Barker, ibid., **46**, 970 (1934).

4) E. K. Plyler and E. F. Barker, *J. Chem. Phys.*, **3**, 367 (1935).

5) H. H. Nielsen and A. H. Nielsen, *Phys. Rev.*, **56**, 274 (1939); **68**, 99 (1954); *Rev. Mod. Phys.*, **16**, 241 (1944).

6) B. T. Darling and D. M. Dennison, *Phys. Rev.*, **57**, 128 (1940).

7) H. D. Noether, *J. Chem. Phys.*, **10**, 664 (1942).

8) R. T. Lageman and H. H. Nielsen, ibid., **10**, 668 (1942).

9) C. P. Courtoy, *Ann. Soc. Sci. Bruxelles*, **LX**, 122 (1946).

10) F. Halverson, *Rev. Mod. Phys.*, **19**, 87 (1947).

11) M'me R. Mathis Noel, *Compt rend.*, **230**, 2168 (1950). *J. phys. Radium*, **12**, 550 (1951).

12) P. F. Fenlon, F. F. Cleveland and A. G. Meister, *J. Chem. Phys.*, **19**, 156 (1951).

13) I. L. Mador and R. S. Quinn, ibid., **20**, 1837 (1952).

14) R. B. Bernstein, F. F. Cleveland and F. L. Voelz, ibid., **22**, 196 (1954).

15) H. B. Weissman, R. B. Bernstein, S. E. Rosser, A. G. Meister and F. F. Cleveland, *J. Chem. Phys.*, **23**, 544 (1955).

16) F. A. Andersen, Private communication.

17) W. F. Edgell and L. Parts, *J. Am. Chem. Soc.*, **77**, 5515 (1955).

18) J. D. Cox, M. S. Tunner and R. J. Warner, *J. Chem. Soc.*, **1950**, 3167.

CH_3X, CD_3OH, HX, etc.) was not detected in their infrared spectra.

Spectrometer.—A Perkin-Elmer 112G grating infrared spectrometer was used throughout the investigation. CH_3X and CD_3X fundamentals were observed with a cell 10 cm. long. In the case of CH_3X, a long-path cell (with a net length of about 6 m.) was also used. The pressure of the gas was controlled in each case, ranging from 5 mmHg to some hundreds of mmHg. The resolution of the Perkin-Elmer 112G spectrometer is about 0.6 cm^{-1} at 15 μ and 0.8 cm^{-1} at 3μ. Because the spectrometer has a slingle-beam system, the presence of water and carbon dioxide in the air seriously disturbs the observation. This difficulty was partially removed by an introduction of the stream of air free from water and carbon dioxide into the whole apparatus, but some bands were still obscured by the bands of residual water or carbon dioxide.

Results for the E-type Fundamental Bands

All of the E-type fundamental bands were observed as a series of finely-resolved Q branch subbands, with the intensity alternation to be expected for the C_{3v} symmetric top molecules. As has already been pointed out, the origin of the subband peak (the position corresponding to the $J=K$ of ${}^RQ_K$ and ${}^PQ_K$) should be at the foot of the steeper side of the absorption curve. The observed curves are, however, more or less deformed by the limited resolving power of the instrument, the effect of the slit function, the pressure broadening, and other reasons. Therefore, it is almost impossible to determine the position of the subband origins precisely. The "peak frequencies," namely, the frequencies of the maximum absorption points, were accordingly measured; they correspond to those for J_m in Eq. 24. (See Appendix I)

The criteria for finding the ${}^RQ_0$ for the E-type bands have already been discussed by several authors, especially by Overend and Crawford.[19] In many of the present investigations, however, it was found difficult to apply the method recommended by them, for the bands, the ${}^RQ_0$ of which could not be easily determined, were apparently irregular or in some cases, only half of the members of the series were observed; under such conditions, the measurement and the summing up of the band intensity were impossible. Consequently, the ${}^RQ_0$'s were determined according to the following features of the band:

1) The intensity alternation caused by the statistical spin weight, depending upon the K numbers (strong for the subbands of $K=3m$, weak for $K\neq 3m$, where m is an integer).

2) The gradual increase and decrease in the intensity of the subbands, with a maximum at ${}^RQ_0$ (besides the spin weight mentioned above). There may be the cases where the ${}^RQ_0$ peaks are abruptly weakened in intensity, but the survey of the peak intensities as a whole offers a reliable criterion.

3) The series of the molecules investigated must have parallel spectroscopic natures as the attached halogen atom changes from Cl to Br and to I.

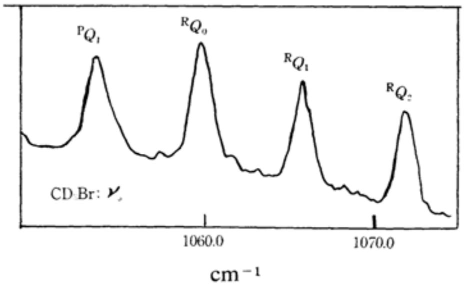

Fig. 1. CD_3Br; Part of ν_5 ($\perp$).

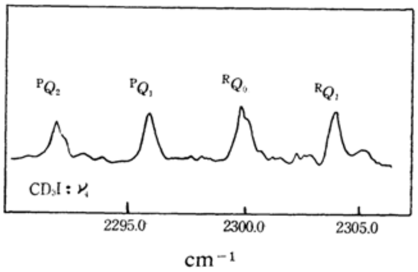

Fig. 2. CD_3I; Part of ν_4 ($\perp$).

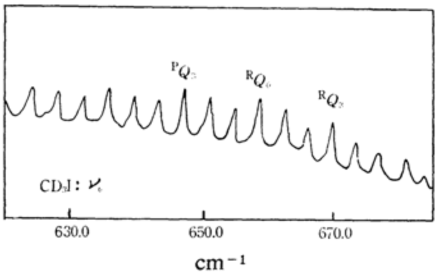

Fig. 3. CD_3I; ν_6 ($\perp$).

Typical absorption curves are shown in Figs. 1—3. Observed peak frequencies and the assignments are listed in columns 2 and 3 of Tables I—XVIII respectively. These values were obtained as the most probable values out of several observations with different conditions. The asterisks in the tables show the peaks which were omitted from the least-squares calculations because they either are obscured by the presence of foreign bands, such as those of carbon dioxide and water, or are at apparently irregular positions.

---

[19] J. Overend and B. Crawford Jr., *J. Chem. Phys.*, 29, 1002 (1958).

If one ignores the effect of the centrifugal distortion and a slight change in the J_m number in the different K subbands, we should be able to fit, the observed peak frequencies to a quadratic equation of K, Eq. 1:

$$\nu^{\mathrm{sub}} = C_0 + C_1 K + C_2 K^2 \qquad (1)$$

and the separations of the successive Q branches ($\Delta\nu_K$) plotted against their K numbers should give a straight line with a tangent twice the coefficient C_2 (Fig. 4). The values of $\Delta\nu_K$ are listed in column 4 of Tables I—XVIII.

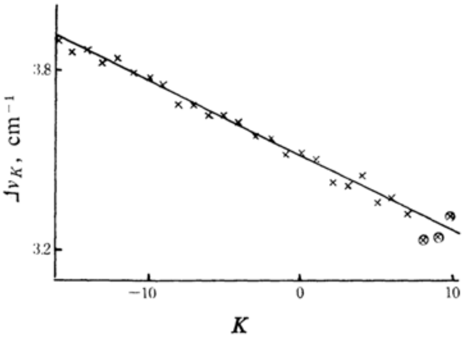

Fig. 4. $\Delta\nu_K = (Q_{K+1} - Q_K)$: CD$_3$Cl : $\nu_4(\perp)$ ⊗: Overlapped with a CO$_2$ absorption.

Some peculiar features observed by the examination of $\Delta\nu_K$'s are as follows:

(i) **The ν_4 Band of CH$_3$Cl.**—Figure 5 shows the irregular nature of the ν_4 band of CH$_3$Cl. As has already been mentioned, each subband the K number of which is a multiple of three has a greater absorption intensity than its neighbors, thus making a series of intensity alternations: strong, weak, weak, strong, etc. In the ν_4 band of CH$_3$Cl, however, the sequence is apparently perturbed at about 3070 cm^{-1}. After a rather regular series of peaks assigned as $^RQ_{12}$—$^RQ_3$, three somewhat deformed and broad peaks follow, with a stronger peak as a fourth, from which another sequence of strong, weak, weak, starts. The separations, $\Delta\nu_K$, also change abruptly in this region, and, moreover, the tangents of the two sequences mentioned above differ beyond the range of error of the measurement. These features clearly show the existence of a certain perturbation which has not been considered before.

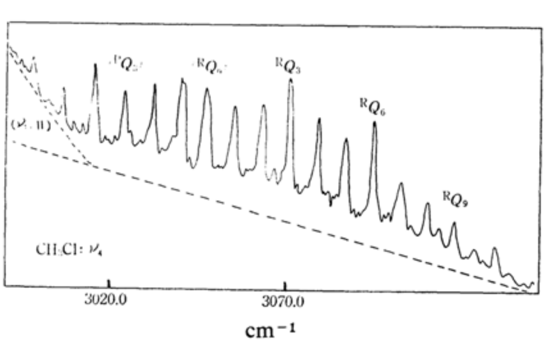

Fig. 5. CH$_3$Cl: ν_4 ($\perp$).

A similar type of irregularity takes place in the combination bands related to ν_4 (the perpendicular band of $2\nu_4$,[20] and $\nu_1+\nu_4$). For the present, the peak at 3071.30 cm^{-1} was assigned

TABLE I. FINE STRUCTURE OF THE ν_4 BAND OF CH$_3$Cl

No.	ν_{obs}	Assignment	$\Delta\nu_K$	ν_{calcd}	$\nu_{\mathrm{obs}} - \nu_{\mathrm{calcd}}$
1	2989.57*	($^PQ_7$)		2987.74	(+1.83)
2	2998.08*	($^PQ_6$)		2995.31	(+2.77)
3	3006.64*	($^PQ_5$)		3003.85	(+2.79)
4	3012.37*	($^PQ_4$)		3012.37	(0.00)
5	3023.84*	($^PQ_3$)		3020.87	(−2.97)
6	3031.86*	($^PQ_2$)		3029.33	(+2.53)
7	3040.26*	($^PQ_1$)		3037.78	(+2.48)
8	3047.41*	$^RQ_0$	7.47	3046.20	(+1.21)
9	3054.88*	$^RQ_1$	8.21	3054.59	(+0.29)
10	3063.09*	$^RQ_2$	8.21	3062.96	(+0.10)
11	3071.30	$^RQ_3$	8.31	3071.30	0.00
12	3079.61	$^RQ_4$	8.27	3079.61	0.00
13	3087.88	$^RQ_5$	8.28	3087.90	−0.02
14	3096.16	$^RQ_6$	8.28	3096.16	0.00
15	3104.44	$^RQ_7$	8.16	3104.40	+0.04
16	3112.60	$^RQ_8$	8.20	3112.62	−0.02
17	3120.80	$^RQ_9$	8.52	3120.80	0.00
18	3129.52*	$^RQ_{10}$	7.99	3128.96	+0.36
19	3137.31*	$^RQ_{11}$	7.99	3137.10	+0.20
20	3145.30*	$^RQ_{12}$		3145.21	+0.09

TABLE II. FINE STRUCTURE OF THE ν_5 BAND OF CH$_3$Cl

No.	ν_{obs}	Assignment	$\Delta\nu_K$	ν_{calcd}	$\nu_{\mathrm{obs}} - \nu_{\mathrm{calcd}}$
1	1386.30*	$^PQ_6$	12.54	1386.02	+0.28
2	1398.84*	$^PQ_5$	12.20	1398.57	+0.27
3	1411.04	$^PQ_4$	12.28	1411.03	+0.01
4	1423.32	$^PQ_3$	12.33	1423.39	−0.07
5	1435.65	$^PQ_2$	12.26	1435.65	0.00
6	1447.91*	$^PQ_1$	11.51	1447.82	+0.09
7	1459.42*	$^RQ_0$	12.49	1459.89	−0.47
8	1471.91	$^RQ_1$	11.84	1471.86	+0.05
9	1483.75	$^RQ_2$	11.70	1483.74	+0.01
10	1495.45	$^RQ_3$	11.68	1495.52	−0.07
11	1507.13	$^RQ_4$	11.67	1507.21	−0.08
12	1518.80	$^RQ_5$	11.58	1518.79	+0.01
13	1530.38	$^RQ_6$	11.21	1530.29	+0.09
14	1541.59*	$^RQ_7$	11.42	1541.68	−0.09
15	1553.01	$^RQ_8$	11.13	1552.99	+0.02
16	1564.14	$^RQ_9$	11.18	1564.19	−0.05
17	1575.32	$^RQ_{10}$	10.98	1575.30	+0.02
18	1586.30	$^RQ_{11}$		1586.31	−0.01

---

[20] R. G. Brown and T. H. Edwards, ibid., **28**, 384 (1958).

TABLE III. FINE STRUCTURE OF THE ν_6 BAND OF CH_3Cl

No.	ν_{obs}	Assignment	$\Delta\nu_K$	ν_{calcd}	$\nu_{obs}-\nu_{calcd}$
1	959.19	$^PQ_9$	6.54	959.20	−0.01
2	965.73	$^PQ_8$	6.63	965.73	0.00
3	972.36	$^PQ_7$	6.57	972.32	+0.04
4	978.93	$^PQ_6$	6.64	978.94	−0.01
5	985.57	$^PQ_5$	6.80	985.62	−0.05
6	992.37	$^PQ_4$	6.73	992.35	+0.02
7	999.10	$^PQ_3$	6.87	999.12	−0.02
8	1005.97	$^PQ_2$	6.90	1005.94	+0.03
9	1012.87	$^PQ_1$	6.83	1012.81	+0.06
10	1019.70	$^RQ_0$	7.01	1019.73	−0.03
11	1026.71	$^RQ_1$	7.05	1026.69	+0.02
12	1033.76	$^RQ_2$	6.93	1033.71	+0.05
13	1040.69	$^RQ_3$	7.13	1040.77	−0.08
14	1047.82	$^RQ_4$	7.25	1047.88	−0.06
15	1055.07	$^RQ_5$	7.13	1055.03	+0.04
16	1062.50	$^RQ_6$	7.30	1062.24	−0.04
17	1069.50	$^RQ_7$	7.33	1069.49	+0.01
18	1076.83	$^RQ_8$	7.18	1076.79	+0.04
19	1084.01	$^RQ_9$	7.54	1084.14	−0.13
20	1091.55	$^RQ_{10}$	7.37	1091.54	+0.01
21	1098.92	$^RQ_{11}$	7.60	1098.98	−0.06
22	1106.52	$^RQ_{12}$		1106.48	+0.04

TABLE IV. FINE STRUCTURE OF THE ν_4 BAND OF CH_3Br

No.	ν_{obs}	Assignment	$\Delta\nu_K$	ν_{calcd}	$\nu_{obs}-\nu_{calcd}$
1	2996.61	$^PQ_7$	9.33	2996.60	+0.01
2	3005.94	$^PQ_6$	9.35	3005.97	−0.03
3	3015.29	$^PQ_5$	9.22	3015.27	+0.02
4	3024.51	$^PQ_4$	9.24	3024.51	0.00
5	3033.75	$^PQ_3$	9.05	3033.69	+0.06
6	3042.80	$^PQ_2$	9.02	3042.80	0.00
7	3051.82	$^PQ_1$	9.00	3051.84	−0.02
8	3060.82	$^RQ_0$	8.89	3060.82	0.00
9	3069.71	$^RQ_1$	8.82	3069.73	−0.02
10	3078.53	$^RQ_2$	8.87	3078.58	−0.05
11	3087.40	$^RQ_3$	8.67	3087.37	+0.03
12	3096.07	$^RQ_4$	8.59	3096.08	−0.01
13	3104.66	$^RQ_5$	8.65	3104.73	−0.07
14	3113.31	$^RQ_6$	8.61	3113.32	−0.01
15	3121.92	$^RQ_7$	8.48	3121.84	+0.08
16	3130.40	$^RQ_8$	8.31	3130.30	+0.10
17	3138.71	$^RQ_9$	8.27	3138.69	+0.02
18	3146.98	$^RQ_{10}$	8.23	3147.01	−0.03
19	3155.21	$^RQ_{11}$	8.00	3155.27	−0.06
20	3163.21*	$^RQ_{12}$	8.23	3163.46	−0.25
21	3171.44*	$^RQ_{13}$		3171.59	−0.15

to $^RQ_3$, because this choice of *K*-numbering seems most reasonable according to the three criteria mentioned above. Three coefficients of Eq. 1 were thus estimated from the data for the bands $^RQ_3$—$^RQ_9$ for convenience.

TABLE V. FINE STRUCTURE OF THE ν_5 BAND OF CH_3Br

No.	ν_{obs}	Assignment	$\Delta\nu_K$	ν_{calcd}	$\nu_{obs}-\nu_{calcd}$
1	1338.56	$^PQ_9$	12.73	1338.38	+0.16
2	1351.29	$^PQ_8$	12.58	1351.21	+0.08
3	1363.87	$^PQ_7$	12.62	1363.94	−0.07
4	1376.49	$^PQ_6$	12.44	1376.57	−0.08
5	1388.93	$^PQ_5$	12.55	1389.11	−0.18
6	1401.48	$^PQ_4$	12.40	1401.55	−0.07
7	1413.88	$^PQ_3$	12.19	1413.89	−0.01
8	1426.07	$^PQ_2$	12.16	1426.13	−0.06
9	1438.23	$^PQ_1$	11.99	1438.28	−0.05
10	1450.22	$^RQ_0$	12.15	1450.33	−0.11
11	1462.37	$^RQ_1$	11.91	1462.28	+0.09
12	1474.28	$^RQ_2$	11.82	1474.14	+0.14
13	1486.10	$^RQ_3$	11.50	1485.90	+0.20
14	1497.60	$^RQ_4$	11.64	1497.57	+0.03
15	1509.24	$^RQ_5$	11.30	1509.13	+0.11
16	1520.54	$^RQ_6$	11.43	1520.60	−0.06
17	1531.97	$^RQ_7$	11.16	1531.97	0.00
18	1543.13	$^RQ_8$	11.26	1543.25	−0.12
19	1554.39	$^RQ_9$	10.86	1554.43	−0.04
20	1565.25*	$^RQ_{10}$	11.40	1565.50	−0.28
21	1576.65*	$^RQ_{11}$	10.23	1576.49	+0.16
22	1586.88*	$^RQ_{12}$		1587.38	+0.50

TABLE VI. FINE STRUCTURE OF THE ν_6 BAND OF CH_3Br

No.	ν_{obs}	Assignment	$\Delta\nu_K$	ν_{calcd}	$\nu_{obs}-\nu_{calcd}$
1	871.86*	$^PQ_{12}$	6.68	871.72	+0.14
2	878.54	$^PQ_{11}$	6.90	878.54	0.00
3	885.44	$^PQ_{10}$	6.89	885.42	+0.02
4	892.33	$^PQ_9$	7.07	892.34	−0.01
5	899.40	$^PQ_8$	6.98	899.33	+0.07
6	906.38	$^PQ_7$	7.01	906.37	+0.01
7	913.39	$^PQ_6$	7.12	913.46	−0.07
8	920.51	$^PQ_5$	7.31	920.61	−0.10
9	927.82	$^PQ_4$	7.25	927.81	+0.01
10	935.07	$^PQ_3$	7.36	935.07	0.00
11	942.43	$^PQ_2$	7.30	942.38	+0.05
12	949.73	$^PQ_1$	7.42	949.74	−0.01
13	957.15	$^RQ_0$	7.49	957.17	−0.02
14	964.64	$^RQ_1$	7.52	964.64	0.00
15	972.16	$^RQ_2$	7.61	972.17	−0.01
16	979.77	$^RQ_3$	7.62	979.76	+0.01
17	987.39	$^RQ_4$	7.75	987.40	−0.01
18	995.14	$^RQ_5$	7.72	995.09	+0.05
19	1002.86	$^RQ_6$	7.78	1002.84	+0.02
20	1010.64	$^RQ_7$	7.86	1010.64	0.00
21	1018.50	$^RQ_8$	7.96	1018.50	0.00
22	1026.46	$^RQ_9$	7.90	1026.42	+0.04
23	1034.36	$^RQ_{10}$	7.95	1034.38	−0.02
24	1042.31*	$^RQ_{11}$	8.00	1042.41	−0.10
25	1050.31*	$^RQ_{12}$		1050.40	−0.09

TABLE VII. FINE STUCTURE OF THE ν_4 BAND OF CH_3I

No.	ν_{obs}	Assignment	$\Delta\nu_K$	ν_{calcd}	$\nu_{\text{obs}}-\nu_{\text{calcd}}$
1	2999.66	$^{P}Q_7$	9.40	2999.50	+0.16
2	3009.06	$^{P}Q_6$	9.38	3009.04	+0.02
3	3018.44	$^{P}Q_5$	9.36	3018.51	−0.07
4	3027.80	$^{P}Q_4$	9.43	3027.90	−0.10
5	3037.23	$^{P}Q_3$	9.25	3037.23	0.00
6	3046.48	$^{P}Q_2$	9.09	3046.49	−0.01
7	3055.57	$^{P}Q_1$	9.19	3055.68	−0.11
8	3064.76	$^{R}Q_0$	9.05	3064.81	−0.05
9	3073.81	$^{R}Q_1$	9.06	3073.86	−0.05
10	3082.87	$^{R}Q_2$	8.99	3082.84	+0.03
11	3091.86	$^{R}Q_3$	8.79	3091.75	+0.11
12	3100.65	$^{R}Q_4$	8.71	3100.59	+0.06
13	3109.36	$^{R}Q_5$	8.81	3109.37	−0.01
14	3118.17	$^{R}Q_6$	8.55	3118.07	+0.10
15	3126.72	$^{R}Q_7$	8.60	3126.71	+0.01
16	3135.32	$^{R}Q_8$	8.48	3135.27	+0.05
17	3143.80	$^{R}Q_9$	8.39	3143.77	+0.03
18	3152.19	$^{R}Q_{10}$	8.25	3152.20	−0.01
19	3160.44	$^{R}Q_{11}$	8.40	3160.56	−0.12
20	3168.84	$^{R}Q_{12}$		3168.84	0.00

TABLE VIII. FINE STRUCTURE OF THE ν_5 BAND OF CH_3I

No.	ν_{obs}	Assignment	$\Delta\nu_K$	ν_{calcd}	$\nu_{\text{obs}}-\nu_{\text{calcd}}$
1	(1299.77)				
2	(1311.95)				
3	(1323.96)				
4	(1335.42)				
5	(1346.50)				
6	(1356.97)				
7	(1366.98)				
8	(1376.12)				
9	1377.73*	$^{P}Q_6$	10.32		
10	(1384.68)				
11	1388.05*	$^{P}Q_5$	11.01		
12	(1393.07)				
13	1399.06*	$^{P}Q_4$	11.29		
14	(1401.55)				
15	1410.35*	$^{P}Q_3$	11.64		
16	1421.99*	$^{P}Q_2$	11.83		
17	1433.82*	$^{P}Q_1$	11.63		
18	1445.45*	$^{R}Q_0$	12.16		
19	1457.61*	$^{R}Q_1$	11.46		
20	1469.07	$^{R}Q_2$	11.94	1469.09	−0.02
21	1481.01	$^{R}Q_3$	11.84	1480.99	+0.02
22	1492.85	$^{R}Q_4$	11.58	1492.78	+0.07
23	1504.43	$^{R}Q_5$	11.58	1504.47	−0.04
24	1516.01	$^{R}Q_6$	11.46	1516.05	−0.06
25	1527.47	$^{R}Q_7$	11.49	1527.53	−0.06
26	1538.96	$^{R}Q_8$	11.22	1539.00	−0.04
27	1550.18	$^{R}Q_9$	11.15	1550.16	+0.02
28	1561.33	$^{R}Q_{10}$	11.07	1561.32	+0.01
29	1572.40	$^{R}Q_{11}$	10.90	1572.38	+0.02
30	1583.30	$^{R}Q_{12}$		1583.32	−0.02

( ): Peaks of the $(\nu_3+\nu_6)$ band.

TABLE IX. FINE STRUCTURE OF THE ν_6 BAND OF CH_3I

No.	ν_{obs}	Assignment	$\Delta\nu_K$	ν_{calcd}	$\nu_{\text{obs}}-\nu_{\text{calcd}}$
1	825.83*	$^{P}Q_8$	7.29	825.91	−0.08
2	833.12	$^{P}Q_7$	7.27	833.12	0.00
3	840.39	$^{P}Q_6$	7.35	840.39	0.00
4	847.74	$^{P}Q_5$	7.39	847.72	+0.02
5	855.13	$^{P}Q_4$	7.43	855.13	0.00
6	862.56	$^{P}Q_3$	7.57	862.60	−0.04
7	870.13	$^{P}Q_2$	7.61	870.14	−0.01
8	877.74	$^{P}Q_1$	7.69	877.75	−0.01
9	885.43	$^{R}Q_0$	7.73	885.42	+0.01
10	893.16	$^{R}Q_1$	7.83	893.16	0.00
11	900.99	$^{R}Q_2$	7.83	900.97	+0.02
12	908.82	$^{R}Q_3$	7.95	908.84	−0.02
13	916.77	$^{R}Q_4$	8.06	916.78	−0.01
14	924.83	$^{R}Q_5$	8.04	924.79	+0.04
15	932.87	$^{R}Q_6$	8.15	932.87	0.00
16	941.02	$^{R}Q_7$	8.18	941.01	+0.01
17	949.20	$^{R}Q_8$	8.28	949.22	−0.02
18	957.48	$^{R}Q_9$	8.05	957.49	−0.01
19	965.53*	$^{R}Q_{10}$		965.84	−0.31

TABLE X. FINE STRUCTURE OF THE ν_4 BAND OF CD_3Cl

No.	ν_{obs}	Assignment	$\Delta\nu_K$	ν_{calcd}	$\nu_{\text{obs}}-\nu_{\text{calcd}}$
1	2225.15	$^{P}Q_{16}$	3.89	2225.11	+0.04
2	2229.04	$^{P}Q_{15}$	3.86	2229.03	+0.01
3	2232.90	$^{P}Q_{14}$	3.87	2232.92	−0.02
4	2236.77	$^{P}Q_{13}$	3.82	2236.78	−0.01
5	2240.59	$^{P}Q_{12}$	3.84	2240.62	−0.03
6	2244.43	$^{P}Q_{11}$	3.79	2244.43	0.00
7	2248.22	$^{P}Q_{10}$	3.77	2248.22	0.00
8	2251.99	$^{P}Q_9$	3.76	2251.99	0.00
9	2255.75	$^{P}Q_8$	3.68	2255.73	+0.02
10	2259.43	$^{P}Q_7$	3.69	2259.44	−0.01
11	2263.12	$^{P}Q_6$	3.65	2263.13	−0.01
12	2266.77	$^{P}Q_5$	3.65	2266.80	−0.03
13	2270.42	$^{P}Q_4$	3.64	2270.43	−0.01
14	2274.06	$^{P}Q_3$	3.59	2274.05	+0.01
15	2277.65	$^{P}Q_2$	3.57	2277.64	+0.01
16	2281.22	$^{P}Q_1$	3.52	2281.20	+0.02
17	2284.74	$^{R}Q_0$	3.53	2284.74	0.00
18	2288.27	$^{R}Q_1$	3.52	2288.26	+0.01
19	2291.79	$^{R}Q_2$	3.42	2291.74	+0.05
20	2295.21	$^{R}Q_3$	3.41	2295.21	0.00
21	2298.62	$^{R}Q_4$	3.45	2298.65	−0.03
22	2302.07	$^{R}Q_5$	3.37	2302.06	+0.01
23	2305.44	$^{R}Q_6$	3.37	2305.45	−0.01
24	2308.81	$^{R}Q_7$	3.33	2308.81	0.00
25	2312.14	$^{R}Q_8$	3.23	2312.15	−0.01
26	2315.37*	$^{R}Q_9$	3.25	2315.47	−0.10
27	2318.62*	$^{R}Q_{10}$	3.32	2318.76	−0.14
28	2321.94*	$^{R}Q_{11}$	3.17	2322.02	−0.08
29	2325.11*	$^{R}Q_{12}$	3.30	2325.26	−0.15
30	2328.41*	$^{R}Q_{13}$	3.22	2328.47	−0.06
31	2331.63*	$^{R}Q_{14}$	2.87	2331.66	−0.03
32	2334.50*	$^{R}Q_{15}$		2334.82	−0.32

TABLE XI. FINE STRUCTURE OF THE ν_5 BAND OF CD_3Cl

No.	ν_{obs}	Assign-ment	$\Delta\nu_K$	ν_{calcd}	$\nu_{obs}-\nu_{calcd}$
1	1045.97*	${}^PQ_3$	5.94	1045.30	+0.67
2	1051.91*	${}^PQ_2$	6.22	1051.63	+0.28
3	1058.13*	${}^PQ_1$	5.91	1057.91	+0.22
4	1064.04*	${}^RQ_0$	6.29	1064.15	−0.11
5	1070.33	${}^RQ_1$	6.24	1070.35	−0.02
6	1076.57	${}^RQ_2$	6.04	1076.51	+0.06
7	1082.61	${}^RQ_3$	6.07	1082.63	−0.02
8	1088.68	${}^RQ_4$	6.02	1088.70	−0.02
9	1094.70	${}^RQ_5$	6.03	1094.74	−0.04
10	1100.73	${}^RQ_6$	5.95	1100.73	0.00
11	1106.68	${}^RQ_7$	5.92	1106.68	0.00
12	1112.60	${}^RQ_8$	5.94	1112.59	+0.01
13	1118.54	${}^RQ_9$	5.81	1118.46	+0.08
14	1124.35	${}^RQ_{10}$	5.70	1124.29	+0.06
15	1130.05	${}^RQ_{11}$	5.70	1130.08	−0.03
16	1135.75	${}^RQ_{12}$	5.74	1135.82	−0.07
17	1141.49	${}^RQ_{13}$	5.73	1141.52	−0.03
18	1147.22	${}^RQ_{14}$	5.60	1147.19	+0.03
19	1152.82	${}^RQ_{15}$	5.42	1152.81	+0.01
20	1158.24*	${}^RQ_{16}$			

TABLE XII. FINE STRUCTURE OF THE ν_6 BAND OF CD_3Cl

No.	ν_{obs}	Assign-ment	$\Delta\nu_K$	ν_{calcd}	$\nu_{obs}-\nu_{calcd}$
1	736.19	${}^PQ_{10}$	3.21	736.19	0.00
2	739.40	${}^PQ_9$	3.17	739.38	+0.02
3	742.57	${}^PQ_8$	3.26	742.58	−0.01
4	745.83	${}^PQ_7$	3.22	745.81	+0.02
5	749.05	${}^PQ_6$	3.19	749.05	0.00
6	752.24	${}^PQ_5$	3.32	752.31	−0.07
7	755.55	${}^PQ_4$	3.38	755.60	−0.05
8	758.93	${}^PQ_3$	3.37	758.90	+0.03
9	762.30	${}^PQ_2$	3.28	762.22	+0.08
10	765.58	${}^PQ_1$	3.41	765.57	+0.01
11	768.99	${}^RQ_0$	3.32	768.93	+0.06
12	772.31	${}^RQ_1$	3.38	772.31	0.00
13	775.69	${}^RQ_2$	3.40	775.72	−0.03
14	779.09	${}^RQ_3$	3.48	779.14	−0.05
15	782.57	${}^RQ_4$	3.48	782.58	−0.01
16	786.05	${}^RQ_5$	3.44	786.04	+0.01
17	789.49	${}^RQ_6$	3.55	789.52	−0.03
18	793.04	${}^RQ_7$	3.52	793.03	+0.01
19	796.56	${}^RQ_8$	3.51	796.55	+0.01
20	800.07	${}^RQ_9$	3.59	800.09	−0.02
21	803.66	${}^RQ_{10}$	3.77	803.65	+0.01
22	807.43*	${}^RQ_{11}$		807.23	+0.20

(ii) The ν_5 Band of CH_3I.—In the region from 1300 to 1600 cm^{-1}, two series of absorbing peaks were observed. One series, which was assigned to the fundamental band ν_5 covers the region from 1378 to 1585 cm^{-1}. The $\Delta\nu_K$'s for this series, shown in Fig. 6 as

TABLE XIII. FINE STRUCTURE OF THE ν_4 BAND OF CD_3Br

No.	ν_{obs}	Assign-ment	$\Delta\nu_K$	ν_{calcd}	$\nu_{obs}-\nu_{calcd}$
1	2239.17*	${}^PQ_{15}$	4.22	2239.23	+0.06
2	2243.39	${}^PQ_{14}$	4.04	2243.32	+0.07
3	2247.43	${}^PQ_{13}$	4.01	2247.38	+0.05
4	2251.44	${}^PQ_{12}$	4.00	2251.42	+0.02
5	2255.44	${}^PQ_{11}$	3.95	2255.43	+0.01
6	2259.39	${}^PQ_{10}$	3.95	2259.41	−0.02
7	2263.34	${}^PQ_9$	3.89	2263.37	−0.03
8	2267.23	${}^PQ_8$	3.94	2267.30	−0.07
9	2271.17	${}^PQ_7$	3.89	2271.21	−0.04
10	2275.06	${}^PQ_6$	3.87	2275.09	−0.03
11	2278.93	${}^PQ_5$	3.83	2278.94	−0.01
12	2282.76	${}^PQ_4$	3.78	2282.77	−0.01
13	2286.54	${}^PQ_3$	3.76	2286.57	−0.03
14	2290.30	${}^PQ_2$	3.74	2290.34	−0.04
15	2294.04	${}^PQ_1$	3.76	2294.09	−0.05
16	2297.80	${}^RQ_0$	3.74	2297.82	−0.02
17	2301.54	${}^RQ_1$	3.69	2301.52	+0.02
18	2305.23	${}^RQ_2$	3.66	2305.10	+0.04
19	2308.89	${}^RQ_3$	3.62	2308.83	+0.06
20	2312.51	${}^RQ_4$	3.56	2312.45	+0.06
21	2316.07	${}^RQ_5$	3.55	2316.05	+0.02
22	2319.62	${}^RQ_6$	3.59	2319.61	+0.01
23	2323.21	${}^RQ_7$	3.53	2323.15	+0.06
24	2326.74	${}^RQ_8$	3.45	2326.67	+0.07
25	2330.19	${}^RQ_9$	3.46	2330.16	+0.03
26	2333.65	${}^RQ_{10}$	3.37	2333.62	+0.03
27	2337.02	${}^RQ_{11}$	3.38	2337.06	−0.04
28	2340.40	${}^RQ_{12}$	3.39	2340.47	−0.07
29	2343.79	${}^RQ_{13}$		2343.86	−0.07

TABLE XIV. FINE STRUCTURE OF THE ν_5 BAND OF CD_3Br

No.	ν_{obs}	Assign-ment	$\Delta\nu_K$	ν_{calcd}	$\nu_{obs}-\nu_{calcd}$
1	1015.24	${}^PQ_7$	6.44	1015.17	+0.07
2	1021.68	${}^PQ_6$	6.40	1021.59	+0.09
3	1028.08	${}^PQ_5$	6.32	1028.03	+0.05
4	1034.40	${}^PQ_4$	6.37	1034.45	−0.05
5	1040.77	${}^PQ_3$	6.36	1040.83	−0.06
6	1047.13	${}^PQ_2$	6.31	1047.18	−0.05
7	1053.44	${}^PQ_1$	6.10	1053.50	−0.06
8	1059.54*	${}^RQ_0$	6.46	1059.79	−0.25
9	1066.00*	${}^RQ_1$	6.29	1066.04	−0.04
10	1072.29	${}^RQ_2$	6.22	1072.27	+0.02
11	1078.51	${}^RQ_3$	6.13	1078.47	+0.04
12	1084.64	${}^RQ_4$	6.14	1084.63	+0.01
13	1090.78	${}^RQ_5$	6.10	1090.77	+0.01
14	1096.88	${}^RQ_6$	6.05	1096.87	+0.01
15	1102.93	${}^RQ_7$	6.00	1102.94	−0.01
16	1108.93	${}^RQ_8$	6.02	1108.98	−0.05
17	1114.95	${}^RQ_9$	5.99	1114.99	−0.04
18	1120.94	${}^RQ_{10}$	5.96	1120.97	−0.03
19	1126.90	${}^RQ_{11}$	5.95	1126.92	−0.02
20	1132.85	${}^RQ_{12}$	5.79	1132.83	+0.02
21	1138.64*	${}^RQ_{13}$		1138.72	−0.08

TABLE XV. FINE STRUCTURE OF THE ν_6 BAND OF CD_3Br

No.	ν_{obs}	Assign-ment	$\Delta\nu_K$	ν_{calcd}	$\nu_{obs}-\nu_{calcd}$
1	671.40*	$^PQ_{12}$	3.32	671.57	−0.17
2	674.72*	$^PQ_{11}$	3.75	675.03	−0.31
3	678.47*	$^PQ_{10}$	3.62	678.51	−0.04
4	682.09	$^PQ_9$	3.49	682.02	+0.07
5	685.58	$^PQ_8$	3.49	685.55	+0.03
6	689.07	$^PQ_7$	3.60	689.10	−0.03
7	692.67	$^PQ_6$	3.56	692.67	0.00
8	696.23	$^PQ_5$	3.61	696.27	−0.04
9	699.84	$^PQ_4$	3.65	699.88	−0.04
10	703.49	$^PQ_3$	3.71	703.53	−0.04
11	707.20	$^PQ_2$	3.66	707.19	+0.01
12	710.86	$^PQ_1$	3.73	710.88	−0.02
13	714.59	$^RQ_0$	3.71	714.59	0.00
14	718.30	$^RQ_1$	3.78	718.32	−0.02
15	722.08	$^RQ_2$	3.77	722.08	0.00
16	725.85	$^RQ_3$	3.78	725.85	0.00
17	729.63	$^RQ_4$	3.88	729.65	−0.02
18	733.51	$^RQ_5$	3.83	733.48	+0.03
19	737.34	$^RQ_6$	3.90	737.33	+0.01
20	741.24	$^RQ_7$	3.89	741.19	+0.05
21	745.13	$^RQ_8$	3.88	745.09	+0.04
22	749.01	$^RQ_9$	3.94	749.00	+0.01
23	752.95	$^RQ_{10}$	3.95	752.94	+0.01
24	756.90	$^RQ_{11}$	3.94	756.90	0.00
25	760.84	$^RQ_{12}$	4.02	760.88	−0.04
26	764.86	$^RQ_{13}$		764.89	−0.03

TABLE XVI. FINE STRUCTURE OF THE ν_4 BAND OF CD_3I

No.	ν_{obs}	Assign-ment	$\Delta\nu_K$	ν_{calcd}	$\nu_{obs}-\nu_{calcd}$
1	2264.55	$^PQ_9$	4.02	2264.52	+0.03
2	2268.57	$^PQ_8$	3.98	2268.57	0.00
3	2272.55	$^PQ_7$	4.05	2272.61	−0.06
4	2276.60	$^PQ_6$	4.01	2276.61	−0.01
5	2280.61	$^PQ_5$	3.96	2280.59	+0.02
6	2284.57	$^PQ_4$	3.91	2284.54	+0.03
7	2288.48	$^PQ_3$	3.83	2288.46	+0.02
8	2292.31	$^PQ_2$	3.91	2292.35	−0.04
9	2296.22	$^PQ_1$	3.80	2296.21	+0.01
10	2300.02	$^RQ_0$	3.85	2300.05	−0.03
11	2303.87	$^RQ_1$	3.85	2303.86	+0.01
12	2307.72*	$^RQ_2$	3.84	2307.64	+0.08
13	2311.56*	$^RQ_3$		2311.39	+0.17

TABLE XVII. FINE STRUCTURE OF THE ν_5 BAND OF CD_3I

No.	ν_{obs}	Assign-ment	$\Delta\nu_K$	ν_{calcd}	$\nu_{obs}-\nu_{calcd}$
1	975.14*	$^PQ_{12}$	6.48	974.86	+0.28
2	981.62*	$^PQ_{11}$	6.80	981.60	+0.02
3	988.42*	$^PQ_{10}$	6.28	988.30	+0.12
4	994.70*	$^PQ_9$	6.97	994.97	−0.27
5	(996.94)	(Q of $2\nu_3$)			
6	1001.67	$^PQ_8$	6.57	1001.61	+0.06
7	1008.24	$^PQ_7$	6.56	1008.21	+0.03
8	1014.80	$^PQ_6$	6.49	1014.79	+0.01
9	1021.29	$^PQ_5$	6.54	1021.34	−0.05
10	1027.83	$^PQ_4$	6.49	1027.85	−0.02
11	1034.32	$^PQ_3$	6.42	1034.33	−0.01
12	1040.74	$^PQ_2$	6.45	1040.78	−0.04
13	1047.19	$^PQ_1$	6.28	1047.20	−0.01
14	1053.47	$^RQ_0$	6.48	1053.59	−0.12
15	1059.95	$^RQ_1$	6.31	1059.95	0.00
16	1066.26	$^RQ_2$	6.39	1066.28	−0.02
17	1072.65	$^RQ_3$	6.25	1072.57	+0.08
18	1078.90	$^RQ_4$	6.16	1078.83	+0.07
19	1085.06	$^RQ_5$	6.24	1085.07	−0.01
20	1091.30	$^RQ_6$	6.24	1091.27	+0.03
21	1097.54	$^RQ_7$	6.06	1097.44	+0.10
22	1103.60	$^RQ_8$	6.03	1103.58	+0.02
23	1109.63	$^RQ_9$	6.10	1109.68	−0.05
24	1115.73	$^RQ_{10}$	6.08	1115.76	−0.03
25	1121.81	$^RQ_{11}$	5.97	1121.80	+0.01
26	1127.78	$^RQ_{12}$	5.73	1127.82	−0.04
27	1133.51*	$^RQ_{13}$	6.00	1133.80	−0.29
28	1139.51*	$^RQ_{14}$	6.04	1139.75	−0.24
29	1145.55*	$^RQ_{15}$		1145.67	−0.12

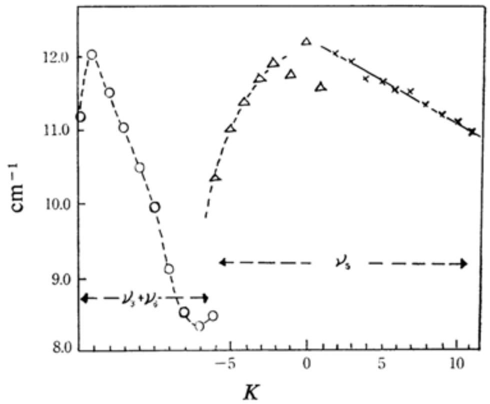

Fig. 6. $\Delta\nu_K=(Q_{K+1}-Q_K)$: CH_3I : ν_5, $\nu_3+\nu_6$.
○, △ Perturbed peaks
× Less perturbed peaks

plotted against K, show a remarkable irregularity; i.e., the tangent of the $\Delta\nu_K$'s for the half of the peaks with larger wave numbers is different in value and opposite in sign from that for the other half of the peaks with smaller wave numbers.

Another series which appears in the region 1300—1400 cm^{-1} is slightly weaker in intensity than the previous one. The strongest peak is at 1356.97 cm^{-1}. A plot of $\Delta\nu_K$ to K gives a straight line with a large tangent, as is shown in Fig. 6. Three peaks in this series (1346.50, 1356.97 and 1366.98 cm^{-1}) coincide with those reported by Bennett and Meyer,[2] Mador and Quinn[13] and Cleveland et al.[14] They did not discriminate these three peaks from those of

TABLE XVIII. FINE STRUCTURE OF THE ν_6 BAND OF CD_3I

No.	ν_{obs}	Assignment	$\Delta\nu_K$	ν_{calcd}	$\nu_{obs}-\nu_{calcd}$
1	616.24*	${}^PQ_{11}$	3.76	616.45	−0.21
2	620.00*	${}^PQ_{10}$	3.68	620.05	−0.05
3	623.68	${}^PQ_9$	3.65	623.67	+0.01
4	627.33	${}^PQ_8$	3.70	627.32	+0.01
5	631.03	${}^PQ_7$	3.67	631.00	−0.03
6	634.70	${}^PQ_6$	3.73	634.71	−0.01
7	638.43	${}^PQ_5$	3.74	638.44	+0.01
8	642.17	${}^PQ_4$	3.80	642.19	−0.02
9	645.97	${}^PQ_3$	3.79	645.97	0.00
10	649.76	${}^PQ_2$	3.85	649.78	−0.02
11	653.61	${}^PQ_1$	3.87	653.62	−0.01
12	657.48	${}^RQ_0$	3.87	657.48	0.00
13	661.35	${}^RQ_1$	3.98	661.37	−0.02
14	665.33	${}^RQ_2$	3.90	665.29	+0.04
15	669.23	${}^RQ_3$	3.98	669.23	0.00
16	673.21	${}^RQ_4$	3.99	673.19	+0.02
17	677.20	${}^RQ_5$	3.97	677.19	+0.01
18	681.17	${}^RQ_6$	4.12	681.21	−0.04
19	685.29	${}^RQ_7$	4.02	685.25	+0.04
20	689.31	${}^RQ_8$	4.12	689.32	−0.01
21	693.43	${}^RQ_9$	4.13	693.42	+0.01
22	697.56	${}^RQ_{10}$	4.15	697.55	+0.01
23	701.71	${}^RQ_{11}$	4.14	701.70	+0.01
24	705.85*	${}^RQ_{12}$	4.08	705.88	−0.03
25	709.93*	${}^RQ_{13}$	4.13	710.08	−0.15
26	714.06*	${}^RQ_{14}$	4.43	714.31	−0.25
27	718.49*	${}^RQ_{15}$	3.82	718.57	−0.08
28	722.31*	${}^RQ_{16}$		722.85	−0.54

ν_5 and treated all peaks as members of ν_5. Lageman and Nielsen[8] also observed the ν_5 band of CH_3I, but they did not extend the region of research beyond 1380 cm^{-1}. This series of subbands, first observed in the present study, should perhaps be assigned to a binary combination band, $\nu_3+\nu_6$ (E). Many other experimental results suggest that the frequency of methyl deformation is in the region from 1440 to 1460 cm^{-1}, and the parallel nature of the methyl halide molecules indicates that the band origin of the ν_5 of CH_3I is at about 1435—1440 cm^{-1}, while the observed values for the fundamental ν_3 and ν_6 of CH_3I are 532.8 and 883.0 cm^{-1} respectively. Consequently, a Fermi resonance is expected between the two vibrational states ν_5 and $\nu_3+\nu_6$. This offers a reasonable explanation for the rather strong absorption intensity of the $\nu_3+\nu_6$ combination band. This type of Fermi resonance is expected, however, only in the case of CH_3I, because, for the other molecules, the separations $\delta=\nu_5-(\nu_3+\nu_6)$ are too large for any appreciable resonance to take place.

There is as yet no satisfactorily rigorous explanation for the anomaly of the rotational fine structures of these bands in terms of the rotational resonance; hence, only half the members of the subbands, ${}^RQ_2$—${}^RQ_{12}$, were used to estimate the coefficients of Eq. 1 for the ν_5 fundamental band. The values thus obtained are not precise. It is, nevertheless, likely that they do not differ very much from the values expected on the basis of the parallelism of six species of methyl halides.

(iii) The Determination of ${}^RQ_0$ of ν_5.—All the ν_5 fundamental bands of the molecules studied were found to be more or less disturbed, so the determinations of K numbers for the observed peaks were difficult. The first unfavorable situation lies in the fact that the centers of the ν_5 and of the ν_2 (CH_3 or CD_3 sym. deform.) bands lie close together. As the absorption range of the ν_5 band usually spreads over 180—250 cm^{-1} because of the wide separations of the Q branches, a part of the ${}^PQ_K$ subbands are more or less overlapped with the strong R branch of the ν_2 band and can, at best, scarcely be observed. This situation occurs most severely in the case of CD_3I, where only three subbands of ${}^PQ_K$ were observed. This is the main reason why the number of the observed peaks is smaller for the ν_5 than for other bands. Secondly, the experimental results show that the ${}^RQ_0$ lines of ν_5 for CH_3Cl, CH_3I, CD_3Cl, CD_3Br and CD_3I are narrower and weaker than expected and that those for CD_3Br and CD_3I are shifted slightly to a longer wavelength side from the expected positions. The reason for this anomaly has not yet been clarified.

Thirdly the shorter wavelength side of the ν_5 band for the CH_3X molecules more or less overlaps with the absorption of water vapor in the air. The overlapping region is the widest in the case of CH_3Cl and the narrowest in CH_3I.

(iv) The ν_5 and $2\nu_3$ Band of CD_3I.—A weak line with its peak at 996.9 cm^{-1} was observed and assigned to the Q branch of $2\nu_3$. As the ν_5 state has the E symmetry and the $2\nu_3$ state, the A symmetry, no coupling is to be expected between the vibrational energy levels of ν_5 and $2\nu_3$. The observed frequencies and the intensities of the neighboring four subbands which belong to ν_5 are, however, perturbed in this region, perhaps through the second-order rotational resonance, and so the data for them were omitted from the least-squares calculation.

(v) A Summary of the Observed Data. — Taking into account the irregularities mentioned above, the coefficients in Eq. 1 were calculated by the least-squares method by using the precisely-determined wave numbers of the subbands. The results may be summarized as follows:

CH_3Cl, ν_4 ; $\nu=3046.20\pm8.405K-0.0128K^2$ (2)

ν_5 ; $\nu=1459.89\pm12.022K-0.0481K^2$ (3)

ν_6 ; $\nu=1019.82\pm6.942K+0.0237K^2$ (4)

CH_3Br, ν_4 ; $\nu=3060.82\pm8.946K-0.0327K^2$ (5)

ν_5 : $\nu=1450.33\pm12.002K-0.0485K^2$ (6)

ν_6 ; $\nu=957.16\pm7.448K+0.0273K^2$ (7)

CH_3I, ν_4 ; $\nu=3064.80\pm9.086K-0.0347K^2$ (8)

ν_5 ; $\nu=1444.98\pm12.162K-0.0527K^2$ (9)

ν_6 ; $\nu=885.42\pm7.707K+0.0335K^2$ (10)

CD_3Cl, ν_4 ; $\nu=2284.74\pm3.527K-0.0125K^2$ (11)

ν_5 ; $\nu=1064.15\pm6.221K-0.0207K^2$ (12)

ν_6 ; $\nu=768.93\pm3.373K+0.0099K^2$ (13)

CD_3Br, ν_4 ; $\nu=2297.82\pm3.710K-0.0130K^2$ (14)

ν_5 ; $\nu=1059.79\pm6.273K-0.0155K^2$ (15)

ν_6 ; $\nu=714.59\pm3.721K+0.0114K^2$ (16)

CD_3I, ν_4 ; $\nu=2300.05\pm3.822K-0.0140K^2$ (17)

ν_5 ; $\nu=1053.59\pm6.373K-0.0156K^2$ (18)

ν_6 ; $\nu=657.48\pm3.875K+0.0131K^2$ (19)

The wave numbers for the subbands calculated by the use of these equations are shown in column 5 of Tables I—XVIII. The differences between the observed and the calculated wave numbers, shown in column 6, are negligibly small.

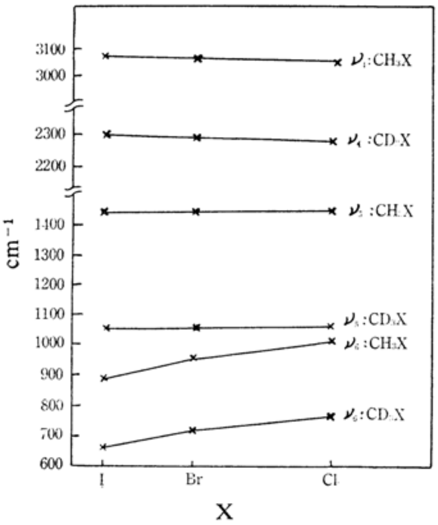

Fig. 7. "Parallel nature" of methyl halides C_0 of Eq. 1.

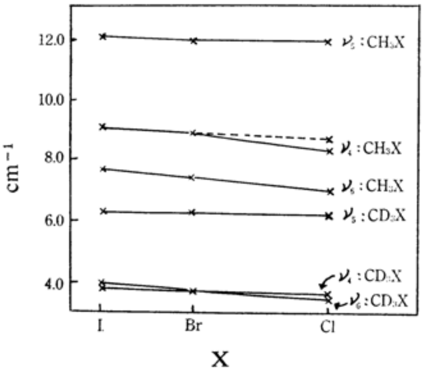

Fig. 8. "Parallel nature" of methyl halides C_1 of Eq. 1.

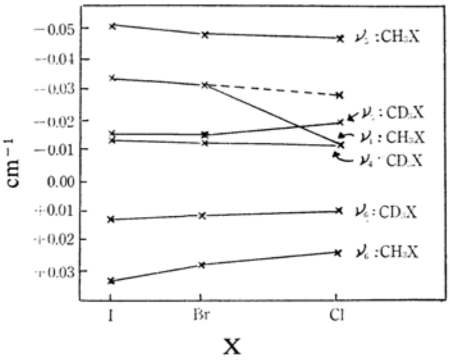

Fig. 9. "Parallel nature" of methyl halides C_2 of Eq. 1.

(vi) The "Parallel Nature" of the Methyl Halide Molecules.—It seems worthwhile to mention here the "parallel nature" of the three coefficients in Eqs. 2—19. As the compounds treated in the present study have a common structure, composed of a methyl group and a halogen atom, their physical constants may be expected to take analogous values with the systematic changes which originate from the nature of the substituents ($H\rightleftharpoons D$ and $X\rightleftharpoons Cl$, Br, and I). Therefore, if a set of three arbitrary positions corresponding to the three halogen atoms (Cl, Br and I) is chosen on the abscissa, and if the coefficients are plotted on the ordinate, they make, as expected, parallel lines, depending on whether they are of CH_3X or of CD_3X type and on the vibrational modes shown in Figs. 7—9. The "parallel nature" of these molecules in the sense noted above was used throughout the present investigation to exclude the uncertainties and apparent irregularities of the data. However, serious deviations from the linear relation always occur for the coefficients of the ν_4 band of CH_3Cl; this fact again suggests that the coefficients in Eq. 2 do not represent the unperturbed state of the ν_4 band. If the parallel nature of the coefficients among the six species is extensively assumed, Eq. 2 might be replaced by Eq. 20 so as to fit the values of the coefficients indicated by the dotted lines in Figs. 8 and 9.

CH_3Cl, ν_4 ; $\nu=3046.20\pm8.720K-0.0290K^2$ (20)

The values for the ν_5 band of CH_3I show an accidental coincidence with the expected linearity, even though they are of a perturbed state.

Coriolis Coupling Constants and Rotational Constants

The vibration-rotation energy levels of a symmetric top molecule in its ground and first-excited states are expressed, to the second order of approximation and by neglecting the effects of centrifugal distortion, by:[21]

$$E_0=W_0+B_0J(J+1)+(A_0-B_0)K^2 \tag{21}$$

for the ground state, and

$$E_v=W_v+B_vJ(J+1)+(A_v-B_v)K^2 \\ -2A_v\zeta_vKl_v+A_v(\zeta_vl_v)^2 \tag{22}$$

for the first excited state, where W denotes the vibrational energies; A and B, the rotational constants about the axes parallel and perpendicular, respectively, to the molecular axis; ζ_v, the effective Coriolis coupling constant of the degenerate mode (see Appendix II), and l_v, the quantum number of the vibrational angular momentum, which is taken as unity for the first excited states of the degenerate vibrations and zero for the non-degenerate vibrations.

The frequencies of the ${}^RQ_K$ or ${}^PQ_K$ subbands are then expressed as follows when the selection rule, $\Delta J=0$ and $\Delta K=\pm1$ is taken into account:

$$\nu=\nu_0+(B_v-B_0)J(J+1)+A_v(1-\zeta_v)^2-B_v \\ \pm2[A_v(1-\zeta_v)-B_v]K+[(A_v-A_0)-(B_v-B_0)]K^2 \tag{23}$$

where the signs + and − before the fourth term refer to the ${}^RQ_K$ and ${}^PQ_K$ branches respectively.

The experimental conditions are such that the actually-observed frequencies are "peak frequencies" which correspond to the maximum absorbing points of the peaks with certain values of J (denoted as J_m). Thus the peak frequencies are expressed as follows:

$$\nu_m=\nu_{0K}+(B_v-B_0)J_m(J_m+1) \tag{24}$$

where

$$\nu_{0K}=\nu_0+A_v(1-\zeta_v)^2-B_v\pm2(A_v(1-\zeta_v)-B_v)K \\ +((A_v-A_0)-(B_v-B_0))K^2 \tag{25}$$

The second term of Eq. 24 has a finite value determined by the Boltzmann distribution and the experimental conditions. It would affect the terms in the expression of ν_{0K} since the J_m is dependent on the K numbers (see Appendix I). Such an effect can, however, be expected to be negligibly small compared with the uncertainty in the measurement of the peak positions, so the second term in Eq. 24 was neglected and the observed data were analyzed according to Eq. 25.

Now the frequencies of the successive Q branches are expressed by the K-dependent equation, the coefficients of which are composed of the molecular parameters, ν_0, A_0, B_0, A_v, B_v and ζ_v. Nevertheless, it is impossible to obtain individual values of these parameters directly from a comparison of Eq. 25 with the observed relations, Eqs. 2—19, because there are more than three unknown parameters. At this stage, therefore, various conventional approximations have been proposed. In the present investigation, two alternative methods were tested.

Method I.—In the first method of approximation, the following assumptions were used in order to minimize the number of unknown molecular parameters:

i) The Coriolis sum rule was approximated as $\zeta_4+\zeta_5+\zeta_6=B_0/2A_0$.[22]

ii) The coefficient of K in Eq. 25 was replaced by $2(A_v-B_0-A_0\zeta_v)$.

iii) The values of B_0 were taken from the data obtained by the analyses of microwave spectra[23] listed in Table XIX.

iv) The term B_v-B_0 was assumed to be zero.

TABLE XIX. THE B_0 VALUES OF METHYL HALIDES (cm^{-1})

	CH_3Cl	CH_3Br	CH_3I	CD_3Cl	CD_3Br	CD_3I
B_0	0.4434	0.3186	0.2502	0.3616	0.2568	0.2015

Assumptions i and ii are made for the sake of simplicity. Assumption iii requires the use of the effective atomic weights of chlorine and bromine since the microwave results are given for isotopic species. As no band splittings were observed for the isotopic species of ${}^{35}Cl$ and ${}^{37}Cl$, nor for those of ${}^{79}Br$ and ${}^{81}Br$, in the degenerate bands, the observed bands of CH_3Cl and CD_3Cl were assigned to those of the ${}^{35}Cl$ species, (accordingly, the B_0 values are those of the ${}^{35}Cl$ species), whereas the B_0 values of methyl bromide were taken as the average of the ${}^{79}Br$ and ${}^{81}Br$ species because the contributions of these two species to the intensities of the absorption bands were expected to be equal in the case of bromides.

By the use of these assumptions, the coefficients of Eqs. 2—19 lead to the values of A_0, A_v, ζ_v and ν_0 shown in Table XX. Set 1 of

---

[21] M. Johnston and D. M. Dennison, *Phys. Rev.*, **48**, 868 (1935); W. H. Shaffer, *J. Chem. Phys.*, **10**, 1 (1940); H. H. Nielsen, *Rev. Mod. Phys.*, **23**, 90 (1951).

[22] F. A. Anderson, B. B. Bak and S. Brodersen, *J. Chem. Phys.*, **24**, 989 (1956).

[23] S. L. Miller, L. C. Aamodt, G. Dousmanis, C. H. Townes and J. Kraitchman, ibid., **20**, 1112 (1952).

TABLE XX. A_0, A_v, ζ_v AND ν_0 VALUES OF METHYL HALIDES (method I)

		A_0 cm^{-1}	A_v cm^{-1}	ζ_v	ν_0 cm^{-1}
CH_3Cl, (1)	ν_4	5.091	5.078	0.085	3042.4
	ν_5		5.043	−0.277	1452.1
	ν_6		5.115	0.236	1017.3
CH_3Cl, (2)	ν_4	5.149	5.120	0.062	3042.1
	ν_5		5.101	−0.263	1452.2
	ν_6		5.173	0.244	1017.3
CD_3Cl	ν_4	2.613	2.600	0.182	2283.4
	ν_5		2.522	−0.337	1059.9
	ν_6		2.623	0.220	767.7
CH_3Br	ν_4	5.123	5.090	0.058	3056.6
	ν_5		5.074	−0.243	1442.8
	ν_6		5.150	0.216	954.3
CD_3Br	ν_4	2.589	2.576	0.179	2296.3
	ν_5		2.574	−0.316	1055.6
	ν_6		2.601	0.187	713.1
CH_3I	ν_4	5.136	5.101	0.060	3060.5
	ν_5		5.083	−0.243	1437.4
	ν_6		5.169	0.208	882.4
CD_3I	ν_4	2.586	2.572	0.178	2298.1
	ν_5		2.570	−0.316	1049.3
	ν_6		2.599	0.178	655.9

CH_3Cl was calculated by the use of Eqs. 2, 3 and 4, and set 2, by the use of Eqs. 3, 4 and 20.

Method II.—It may readily be seen that a more clear-cut treatment is possible if all the rotational correction terms (A_v-A_0) and (B_v-B_0) are known. The knowledge of these values is also indispensable for the determination of the molecular structures at their equilibrium state. Theoretically, the A_v and A_0 are expressed as follows:

$$A_v=A_e-\sum_i \alpha_i(v_i+g_i/2)$$

and

$$A_0=A_e-\sum_i \alpha_i(g_i/2) \tag{26}$$

where α_i is the correction term connected with the ith vibrational mode and is a function of the anharmonic terms in the potential function. Similar relations hold for B_v and B_0 when we replace α_i with β_i. Efforts were also made to obtain information about the values of α_i and β_i. The results obtained to date for the methyl halide molecules are summarized in Table XXI (see Appendix III for the experimental sources). The precise values of A_e and B_e can not be obtained until Table XXI is filled up with appropriate values. However, a close examination of Table XXI suggests the possibility of obtaining rough values of (B_e-B_0) and (A_e-A_0). An interesting relation was obtained when the α_i/A_0 and β_i/B_0 ratios were calculated for all the observed values of α_i and β_i; that is, the ratios are characteristic of the ith vibrational mode and similar for the six species of methyl halides, the deviations being within ±0.1% of A_0 (or B_0). Therefore, the $\sum_i \alpha_i g_i/2$ and $\sum_i \beta_i g_i/2$ sums can be estimated for all the six species by using the observed data of A_0 and B_0, with a possible error of only ±0.6%, if at least six α_i's and six β_i's for the six normal vibrations are known. An estimate was made as follows in the present case:

TABLE XXI. THE OBSERVED VALUES OF α_i AND β_i (cm^{-1})

	CH_3Cl	CH_3Br	CH_3I	CD_3Cl	CD_3Br	CD_3I
α_1	$+0.0547^{a-1}$	+	+	+	+	+
α_2	−	−	−	−	−	−
α_3	+	+	+	+	+	+
α_4	+0.013	+0.033	+0.035	+0.013	+0.013	+0.014
α_5	+0.048	+0.048	+0.055	+0.021	+0.015	+0.016
α_6	−0.024	−0.027	−0.033	−0.010	−0.011	−0.013
β_1	-0.00010^{a-I}					
β_2	$+0.005^{a-I}$					
β_3	$+0.00484^{b-M}$	$+0.0026^{b-M}$	$+0.0018^{c-M}$	$+0.0028^{M}$		
β_4	-0.00022^{d-O}	-0.00008^{e-O}	-0.0001^{e-O}	−	−	−
β_5	-0.0021^{a-O}	−	−	−	−	−
β_6	$+0.001635^{b-M}$	+	+	+	+	+

a = Ref. 26, b = Ref. 24, c = Ref. 25, d = Ref. 20, e = Ref. 27
I = Infrared
M = Microwave
O = Infrared Overtone
others: the present study. See Appendix III.

Note added in proof: Recently the authors have been informed by Dr. E. Jones that all the fundamentals, and many overtones and combination parallel and perpendicular bands of methyl halides have been measured and analyzed at Oxford.

1) As for β's, all six values from β_1 to β_6 are available for CH_3Cl. By the use of these values, B_4, B_5, B_6 and B_e were assumed for all the species as follows:

$$B_4 = B_0(1+0.0005)$$

$$B_5 = B_0(1+0.0048)$$

$$B_6 = B_0(1-0.0037)$$

and

$$B_e = B_0(1+0.0082)$$

where the B_0 values were taken from Table XIX.

2) There is no information about the absolute values of α_2 and α_3. However, an examination of the Q-branch shapes suggests that these terms have almost the same values but opposite signs ($\alpha_2 < 0$, $\alpha_3 > 0$); $\alpha_2+\alpha_3$ was consequently assumed to be zero.

3) The values of α_1 was taken to be 1% of A_0.

4) For α_4, α_5 and α_6, the observed values were used.

5) Assumptions 1 to 4 made it possible to estimate all the necessary values of the rotational constants, if another assumption on the Coriolis sum rule, $\zeta_4+\zeta_5+\zeta_6 = B_e/2A_e$, was made together with Eq. 25.

By using these estimated values, the molecular parameters, A_e, A_0, A_v and ζ_v, of CH_3X and CD_3X can be independently calculated from the observed data of the coefficients C_0, C_1 and C_2. The resultant values of A_e(H) and A_e(D) must satisfy the relation $A_e(\mathrm{H})m_{\mathrm{H}} = A_e(\mathrm{D})m_{\mathrm{D}}$. In the present results, however, the relation did not strictly hold and the deviation from the expected ratio of $A_e(\mathrm{H})/A_e(\mathrm{D})$ was largest for the case 1 of chlorides and was negligibly small for iodides. This inconsistency arose partly because the estimates of (A_e-A_0) and (B_e-B_0) include uncertainties and partly because the experimental data on CH_3X (especially on CH_3Cl) include anomalies, so that the A_e and A_0 values obtained by using these data must be influenced by the anomalies through the Coriolis sum rule used in the analysis.

At present, therefore, the values A_e, A_v, A_0 and ζ_v of CD_3X (of which less anomaly was observed in the spectra) were first determined by the method mentioned above. The A_e(D) values thus obtained were then reduced by the $A_e(\mathrm{H})m_{\mathrm{H}} = A_e(\mathrm{D})m_{\mathrm{D}}$ relation to A_e(H), from which the $B_e/2A_e$ ratio and, henceforth, a set of A_vs and ζ_vs for CH_3X were so determined as to satisfy the Coriolis sum rule, $\zeta_4+\zeta_5+\zeta_6 = B_e/2A_e$. The final results are shown in Table XXII.

TABLE XXII. A_e, A_0, A_v AND ζ_v VALUES OF METHYL HALIDES (method II)

		A_e cm^{-1}	A_0 cm^{-1}	A_v cm^{-1}	ζ_v
CH_3Cl, (1)	ν_4			5.084	0.086
	ν_5	(5.304)	5.148	5.080	−0.278
	ν_6			5.119	0.236
CH_3Cl, (2)	ν_4			5.135	0.065
	ν_5	(5.304)	5.148	5.107	−0.265
	ν_6			5.170	0.243
CD_3Cl	ν_4			2.606	0.184
	ν_5	2.654	2.618	2.599	−0.337
	ν_6			2.627	0.221
CH_3Br	ν_4			5.094	0.059
	ν_5	(5.237)	5.127	5.080	−0.244
	ν_6			5.153	0.216
CD_3Br	ν_4			2.578	0.181
	ν_5	2.620	2.591	2.576	−0.318
	ν_6			2.601	0.186
CH_3I	ν_4			5.107	0.061
	ν_5	(5.228)	5.141	5.090	−0.244
	ν_6			5.174	0.207
CD_3I	ν_4			2.573	0.179
	ν_5	2.616	2.587	2.572	−0.318
	ν_6			2.599	0.177

( ); estimated values: see text.

A comparison of the values in Tables XX and XXII provides the useful suggestion that method I, which is simpler than method II, is a good approximation as far as the determination of ζ_v is concerned. A third, and the simplest, method of analysis is to use the values of A_0 calculated with the structure parameters determined by other experimental methods. This method is, however, less desirable because the uncertainty of A_0 values directly influences the value of ζ_v, and, as will be discussed in the next section, the values of A_0 estimated by the analysis of microwave spectra differ considerably from those of the present investigation.

When all of the ζ_v values can be observed, the use of the Coriolis sum rule has the merit that a set of self-consistent molecular parameters, including the observed values of A_e (or at least A_0), can be obtained from the analysis of the vibration-rotation spectra. An unfavorable point, however, lies in the fact that the irregularity or uncertainty of one vibrational mode affects all the other values through the sum rule, as was observed in the case of CH_3Cl.

The Structures of Methyl Halides

In the preceding section, the rotational constants, A_e, B_e, A_0 and B_0, of the six species of methyl halides were obtained with a number of empirical assumptions and approximations. These rotational constants are related to the moments of inertia, I_a and I_b, about the axes parallel and perpendicular to the molecular axis, respectively, by the equations;

$$A_e = h/(8\pi^2 c I_a{}^e)$$

and

$$B_e = h/(8\pi^2 c I_b{}^e) \tag{27}$$

The terms $I_a{}^e$ and $I_b{}^e$ are, in turn, expressed by the molecular parameters of the equilibrium configuration of the molecule:

$$\begin{aligned} I_a{}^e &= 2m_{\mathrm{H}} r_{\mathrm{H}e}{}^2(1-\cos\theta_e) \\ I_b{}^e &= m_{\mathrm{H}} r_{\mathrm{H}e}{}^2(1-\cos\theta_e) + m_{\mathrm{H}}(m_{\mathrm{C}}+m_{\mathrm{X}}) \\ &\quad \times r_{\mathrm{H}e}{}^2(1+2\cos\theta_e)/M + m_{\mathrm{X}} r_{\mathrm{X}e}[(3m_{\mathrm{H}} \\ &\quad + m_e) r_{\mathrm{X}e} + 6m_{\mathrm{H}} r_{\mathrm{H}e}((1+2\cos\theta_e)/3)^{1/2}]/M \end{aligned} \tag{28}$$

where m_{H}, m_{C} and m_{X} denote the masses of the atoms H, C and X respectively. θ_e is the angle HCH of the equilibrium configuration, and $M = (3m_{\mathrm{H}} + m_{\mathrm{C}} + m_{\mathrm{X}})$ is the total mass of the molecule. Analogous relations hold for A_0 and B_0. It should be noted that A_0 and B_0 include terms originating both from the coupling of vibration and rotation and from the anharmonicity of the potential function. Moreover, they have these terms as a result of taking an average of $1/r^2$ over the ground vibrational state. Thus the determination of the so-called "r_0 structure" is by no means the final goal of our structure determination. However, it seems interesting to compare the r_0 structures of methyl halides estimated from microwave spectra[23] with those estimated by the use of the present A_0 values.

Since there are three unknown parameters, r_{H_0}, r_{X_0} and θ_0, they can not be determined from the A_0 and B_0 values alone. On the other hand, the r_0 structures obtained from microwave spectra depend on the changes in B_0 resulting from the substitution of the isotopes in the molecule, and, although they are uncertain because of the neglect of the changes in the zero-point contributions, the r_{X_0} values are usually determined more precisely than those of r_{H_0} and θ_0. Therefore, the values of r_{X_0} were taken, for the sake of convenience, from the microwave data.[23] Assuming the same values of r_{X_0} for the CH_3X and CD_3X molecules, the other parameters were obtained by the use of the A_0 and B_0 values determined above. The results are shown in Table XXIII, where the values for CH_3Cl(1) and CH_3Cl(2) correspond to the use of Eqs. 2 and 20 respectively.

TABLE XXIII. THE r_0 STRUCTURES OF METHYL HALIDES

	r_{X_0}, Å	PR		M	
		r_{H_0}, Å	θ_0	r_{H_0}, Å	θ_0
CH_3Cl (1)	(1.7810)	1.1050	110°12′	1.113	110°31′
CH_3Cl (2)	(1.7810)	1.0995	110°00′		
CD_3Cl	(1.7810)	1.0912	110°11′	1.104	110°43′
CH_3Br	(1.9391)	1.0978	110°46′	1.113	111°14′
CD_3Br	(1.9391)	1.0908	111°00′	1.104	111°26′
CH_3I	(2.1392)	1.0956	110°53′	1.113	111°25′
CD_3I	(2.1392)	1.0900	111°14′	1.104	111°37′

( ): assumed.
PR: Present investigation.
M: Ref. 23.

The structures proposed by Miller et al.[23] (shown for comparison in columns 2, 5 and 6 of Table XXIII) are those determined on the assumption that the difference $r_{\mathrm{H}_0} - r_{\mathrm{D}_0} = 0.009$ Å for all the pairs of CH_3X and CD_3X, irrespective of the halogen atoms. The results of the present investigation show, however, that the values of $r_{\mathrm{H}_0} - r_{\mathrm{D}_0}$ differ slightly according to the change in halogen atoms if the r_{X} is taken as common for the two species, CH_3X and CD_3X. The absolute values of r_{H} and r_{D} are smaller than those in column 5. As for the bond angles, the conclusion of Miller et al. that the angle HCH is larger than the tetrahedral one was again confirmed. As a whole, the A_0 values estimated by using the r_{H} and θ values by Miller et al. are considerably larger than those observed in the present study.

When the configurations of CH_3X and CD_3X in their equilibrium state is assumed to be the same, the r_e structures of methyl halides are obtained from the values of A_e and B_e without further assumptions, as is shown in Table XXIV.

TABLE XXIV. THE r_e STRUCTURES OF METHYL HALIDES

	$r_{\mathrm{X}e}$, Å	$r_{\mathrm{H}e}$, Å	θ_e
CH_3Cl, CD_3Cl	1.779	1.079	110°43′
CH_3Br, CD_3Br	1.936	1.080	111°35′
CH_3I, CD_3I	2.136	1.079	112°00′

Since the values of A_e and B_e employed are uncertain, these parameters should also include large errors, yet the general tendency, ($r_{\mathrm{X}e} < r_{\mathrm{X}_0}$ and $r_{\mathrm{H}e} < r_{\mathrm{H}0}$) seems reasonable when the anharmonicity of the potential field is thought to have such a form as is expressed by the Morse function. The error of 1% in the A_e value corresponds to the change of ± 0.003 Å in $r_{\mathrm{H}e}$ and that of $\pm 10'$ in θ_e. The effect of the errors in the B_e values should be more serious.

Discussion

The theoretical and numerical calculations of the intramolecular force field using the Coriolis coupling constants[1] have proved that these constants are useful observables for the determination of the force field. This fact, however, means in turn that the experimental values of the Coriolis coupling constants must be determined precisely enough to give a critical check of the force field. The present investigation shows that the accuracy of the observed values of the Coriolis coupling constants is influenced by many factors, such as

1) The accuracy of the spectral measurement,

2) The approximations used in the course of the analysis,

3) The assignment of the K numbering, the existence of the Fermi resonance, and other interactions, and

4) The effect of anharmonicity.

1) The first factor depends almost entirely on the uncertainties of the optical instrument used. The minimum requirement is that the individual Q branches are well resolved and that the accuracy of the measurement of peak frequencies is such that the K-dependence of the successive Q branch separations can be observed. The methyl halide molecules, of which the three off-axial atoms are all hydrogen or all deuterium, have the largest A_0 values among the symmetric top molecules; yet a grating spectrometer of medium dispersion is necessary for the observation of their spectra to satisfy the above requirement.

The maximum uncertainty of the observed frequencies is $\pm 0.1\ \mathrm{cm}^{-1}$. The coefficients of Eqs. 2—20 are determined by the least-squares method, using the observed data, so the accuracy of C_0, C_1 and C_2 in Eq. 1 is a function of the number of observed peaks. The standard deviations of these coefficients are estimated to be of the following orders of magnitude:

$$\sigma(C_0)=\pm 0.05, \qquad \sigma(C_1)=\pm 0.005$$

and $\sigma(C_2)=\pm 0.0005\ \mathrm{cm}^{-1}$

The effect of these deviations on the ζ values is estimated to be less than 0.001.

2) a) "*Peak Frequency.*"—The uncertainties due to the "peak frequency" measurement are discussed in Appendix I. As the final result depends on the slit function of the instrument, the estimation of the error is difficult. The upper limit of the error may, however, be $(B_v-B_0)(kT/hB_0)^{1/2}$ for the C_1 in the case of ${}^{R}Q_0$—${}^{R}Q_n$. This term amounts to $\pm 0.042\ \mathrm{cm}^{-1}$ for the ν_5 band of CD_3Cl, and this leads to an error of -0.008 for ζ_5.

2) b) *The Approximation of* $(\zeta_v^{(z)})'$ *to* $\zeta_v^{(z)}$.—The difference is of the order of 0.004, as will be estimated in Appendix II.

2) c) *The Reducction of the Molecular Parameters from the Observed Coefficients in Eq. 1.*—As the theoretical expression of the subband frequencies (Eq. 25) consists of many molecular parameters, approximations must be introduced so as to determine them by using the observed data. A comparison of two alternative treatments in the preceding section (Tables XX and XXII) will show, however, that the ζ values are little affected by the method of analysis as long as the value (A_v-A_0) is taken into account and the Coriolis sum rule is used. The difference in the ζ's given in Tables XX and XXII is less than 0.003.

3) a) *The Assignment of the K Numbering.*—As has been discussed in the preceding section, the determination of the K numbers in a series of Q branches is very difficult and, therefore, there sometimes remains an ambiguity in the assignment. The change of assignment, however, results in a fairly large variation in the ζ values. Revision of the assignment Q_K to Q_{K+1} leads to the change of C_1 to (C_1-2C_2). The magnitude of C_2 is 0.01—0.05 cm^{-1} for the fundamental bands of methyl halides. (Some of the combination bands have greater C_2 values.) Accordingly, a revision of Q_K to $Q_{K\pm 3}$ (which occurs rather frequently), with large C_2 values, results in a change in ζ of up to ± 0.03.

3) b) *The Effect of Resonance.*— When a series of Q branches is well resolved but has an irregular feature, the existence of rotational resonances must be suspected (e. g., the ν_4 of CH_3Cl and the ν_5 of CH_3I). Complete analyses of such bands have not yet been reported. Therefore, the values can not be determined with certainty. For example, Cleveland et al.[14)] obtained a value of the ζ_5 of CH_3I ($\zeta_5=-0.208$) by making all the data fit a quadratic equation of K with equal weights. The present result ($\zeta_5=-0.244$) is based on the less-perturbed part of the series.

These two factors, a) and b), include errors of an "unknown" order; they may amount to large values if the band in question alone is investigated. In the present investigation, however, the consideration of the "parallel nature" partly excludes such uncertainties, so that the accuracy of the final result may be estimated, after all the factors mentioned are taken into account, to be ± 0.02 in the absolute value of the Coriolis coupling constants.

The last factor, "anharmonicity," represents the question of whether the observed ζ values can be regarded as ζ_e, in other words, whether the Coriolis coupling constants can be expressed by the equations:

$$\zeta=\zeta_e+\sum_{i,j}\Delta\zeta_{ij}(v_i+g_i/2)(v_j+g_j/2) \qquad (29)$$

or

$$\zeta=\zeta_e+\sum_{i}\Delta\zeta_i(v_i+g_i/2) \qquad (29')$$

as in the case of the vibrational or rotational anharmonic terms. This problem has not yet been elucidated either theoretically or experimentally; the discussion will be postponed to our coming paper on the analysis of the combination bands of methyl halides.

Summary

The infrared spectra of CH_3X and CD_3X (X=Cl, Br and I) have been observed with a high-resolution instrument in the region 500—3300 cm^{-1}. The rotational fine structures of all the E-type fundamental bands have been resolved and analyzed, giving the Coriolis coupling constants, the rotational constants and the frequencies of the band origins. The uncertainties of the observed molecular constants have been discussed. On the basis of the observed data for the rotational constants and their changes by the excitation of vibration, the structures of methyl halide molecules have been determined.

The authors are greatly indebted to Dr. Chi Matsumura for his kind help in the course of their experiments. This work was supported by a grant-in-aid for fundamental scientific research from the Ministry of Education, to which the authors' thanks are also due.

Department of Chemistry
Faculty of Science
The University of Tokyo
Hongo, Tokyo

Appendix I

The definition of the "peak frequency" is simply the frequency of the maximum absorption point of a peak. The observed values of individual subbands included in Tables I—XVIII are, as mentioned in the text, the "peak frequencies." Strictly speaking, however, the absolute value of the "peak frequency" is influenced by many factors. A certain peak of the $^{R}Q_K$ or $^{P}Q_K$ of a symmetric top molecule consists of many lines labelled by the J numbers and is located at the position $\nu=\nu_{0K}+(B_v-B_0)J(J+1)$, and the intensity ratio of these lines is given by:

$$\left.\begin{aligned} I_{^{R}Q_K} &\propto 2(2J+1)\frac{(J+1+K)(J-K)}{J(J+1)} \\ &\quad\times e^{-F(J\cdot K)hc/\boldsymbol{k}T} \\ I_{^{P}Q_K} &\propto 2(2J+1)\frac{(J+1-K)(J+K)}{J(J+1)} \\ &\quad\times e^{-F(J\cdot K)hc/\boldsymbol{k}T} \end{aligned}\right\} \qquad (30)$$

Cleveland et al.[14) applied these relations directly to the case of methyl halides and gave J_{max} values which depend on the K numbers of the subbands and the rotational constants of the molecule. Such a treatment is, however, correct only if the individual lines of different J numbers are resolved.

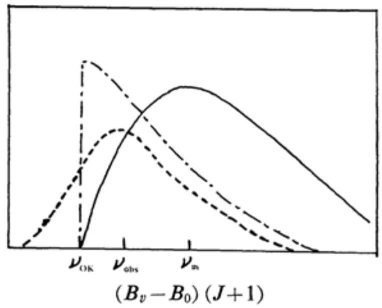

Fig. 10. E type $^{R}Q_0$ branch (schematic).
———: Intensity distribution by Eq. 30
-·-·-: "Averaged" intensity distribution by Eq. 31
------: Observed (re-averaged over the slit function)

In the case of a lower dispersion, the intensity of the lines are averaged over the unequal separations of successive J number lines $((B_v-B_0)\times(2J+1))$, and, accordingly, the $(2J+1)$ factor of Eq. 30 must be dropped out (See Fig. 10). Thus, the "averaged intensity" is expressed as follows:

$$\left.\begin{aligned} I_{av}(^{R}Q_K) &\propto \frac{2(J+1+K)(J-K)}{J(J+1)} \\ &\quad\times e^{-F(J\cdot K)hc/\boldsymbol{k}T} \\ I_{av}(^{P}Q_K) &\propto \frac{2(J+1-K)(J+K)}{J(J+1)} \\ &\quad\times e^{-F(J\cdot K)hc/\boldsymbol{k}T} \end{aligned}\right\} \qquad (31)$$

The K-dependence of the J_m number for the maximum intensity in Eq. 24 can be derived, after the differentiation of Eq. 31, as:

$$\begin{aligned} J_m(J_m+1) &= (\boldsymbol{k}T/hB_0)^{1/2}(K(K+1))^{1/2} \\ &\quad+(1/2)K(K+1) \end{aligned} \qquad (32)$$

The "peak frequency" in the sense of Eq. 31 is given, instead of as Eq. 24, as follows:

$$\begin{aligned} ^{R}Q_K:\ \nu &= \nu_0+(A_v(1-\zeta_v)^2-B_v)+2(A_v(1-\zeta_v)-B_v)K \\ &\quad+((A_v-A_0)-(B_v-B_0))K^2 \\ &\quad+(B_v-B_0)((\boldsymbol{k}T/hB_0)^{1/2}(K(K+1))^{1/2} \\ &\quad+(1/2)K(K+1)) \\ &= \nu_0+(A_v(1-\zeta_v)^2-B_v)+2(A_v(1-\zeta_v) \\ &\quad-B_0-(3/4)(B_v-B_0))K+((A_v-A_0) \\ &\quad-1/2(B_v-B_0))K^2+(B_v-B_0)(\boldsymbol{k}T/hB_0)^{1/2} \\ &\quad\times(K(K+1))^{1/2} \end{aligned} \qquad (33)$$

The expression for the $^{P}Q_K$ is consistent with that for the $^{R}Q_K$ when $(K+1)$ is replaced by $(K-1)$, except for the sign of the last term. These equations may be visualized thus: the "peak" of the E-type subbands is shifted towards the lower or higher frequency, depending on whether the sign of (B_v-B_0) is negative or positive, and the magnitude of the shift is nearly proportional to $|K|$. The separations of the successive Q branches plotted against their K numbers will, in this case, not lie on a straight line but have a break around the band center, as Fig. 11 shows. The conventional

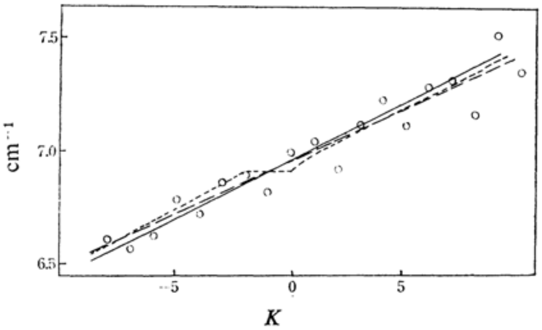

Fig. 11. Effect of the "peak-frequency" measurement.

$\Delta\nu_K = (Q_{K+1} - Q_K)$: CH$_3$Cl : ν_6

——: From the subband origin ν_{0K} of Eq. 25

----: From the "peak frequency" ν_m of Eq. 24

—·—: Least-squares fit of the observed data to Eq. 1

○ : Observed

fitting of the "peak frequencies" to the quadratic equation of K, as was made in the preceding section, will result in small uncertainties for the three coefficients, C_0, C_1 and C_2, of Eq. 1, and the magnitude of the errors depends on the numbers of the observed subbands. For example, the observation of the ${}^RQ_n$ to ${}^PQ_n$ subbands leads to the errors of:

$(3/16)(B_v - B_0)(kT/hB_0)^{1/2} n$ for C_0

0 for C_1 and

$(kT/hB_0)^{1/2}/(K+1/2)$ for C_2.

In another case, that of ${}^RQ_0$ to ${}^RQ_n$, the errors are:

0 for C_0

$(kT/hB_0)^{1/2}$ for C_1 and

0 for C_2.

The above discussion must, however, be again modified when the slit function of the instrument is taken into account. An optimistic expectation is that the effect of the last term in Eq. 33 will be made much smaller after the re-average of the band intensity over the slit function is made. Practically speaking, the dispersions of the observed "peak frequencies" are comparable to or greater than the estimated theoretical "errors," as is shown in Fig. 11; therefore, the contribution of the "peak" measurement is disregarded in the present investigation. The cited values of ν_0 do not include such corrections; corrections of ± 0—$0.4\,\mathrm{cm}^{-1}$ should be added to those ν_0 values where the upper sign is for the band origins of ν_4 and ν_5, and the lower sign, for the ν_6.

Appendix II

According to Nielsen,[21] the energy level of a symmetric top molecule can be expressed as follows:

$$E/hc = W_v + B_v J(J+1) + (A_v - B_v)K^2 \mp 2\tilde{A}_v\left(\sum l_v \zeta_v^{(z)}\right)K \qquad (34)$$

where W_v is the vibrational energy; A_v and B_v are the rotational constants about the axes parallel and perpendicular to the molecular axis respectively; z denotes the direction parallel to the molecular axis; and J and K are the rotational quantum numbers. A_v, $\tilde{A}_v$ and B_v have the following expressions:

$$A_v = A_e - \sum_{s\sigma} \alpha_{s\sigma}(v_s + g_s/2)$$

$$\tilde{A}_v = A_e - \sum_{s\sigma} \tilde{\alpha}_{s\sigma}(v_s + g_s/2)$$

$$B_v = B_e - \sum_{s\sigma} \beta_{s\sigma}(v_s + g_s/2)$$

$$A_e = h/(8\pi^2 c I_a^e)$$

$$B_e = h/(8\pi^2 c I_b^e)$$

$$\tilde{\alpha}_{s\sigma} = \alpha_{s\sigma} + 2\sum_{s'\sigma'} A_e(A_e/g_s\omega_s) \times [(3\lambda_s + \lambda_s')/(\lambda_s - \lambda_s')](\zeta_{s\sigma s'\sigma'}^{(z)})^2 \qquad (35)$$

where the $\alpha_{s\sigma}$ and $\beta_{s\sigma}$ are correction terms to A_v and B_v respectively, and v_s and g_s are the quantum number and the degeneracy of the s-th vibrational mode respectively.

Since the terms A_v and $\tilde{A}_v$ differ slightly from each other, $\zeta_v^{(z)}$ must be modified to $(\zeta_v^{(z)})'$ if Eq. 34 is rewritten in such a way as to include only A_v and B_v as the rotational constants:

$$E/hc = W_v + B_v(J+1)J + (A_v - B_v)K^2 \mp 2A_v\left(\sum l_v (\zeta_v^{(z)})'\right)K \qquad (34')$$

$$(\zeta_v^{(z)})' = \zeta_v^{(z)}\Big[1 - 2\sum_{s\sigma}\sum_{s'\sigma'}(A_e/g_s\omega_s) \times ((3\lambda_s + \lambda_s')/(\lambda_s - \lambda_s'))(\zeta_{s\sigma s'\sigma'}^{(z)})^2(v_s + g_s/2)\Big] \qquad (36)$$

The non-vanishing elements of $\zeta_{s\sigma s'\sigma'}^{(z)}$ are, in the case of methyl hadides, as follows:

$$\zeta_{4a5b}^{(z)},\ \zeta_{4a6b}^{(z)},\ \zeta_{5a6b}^{(z)} \neq 0$$

Accordingly, a numerical calculation shows that the second term in the brackets of Eq. 36 amounts, for example, to 0.004 in the case of the ζ_4 of CH$_3$Cl; therefore, the difference between $\zeta_v^{(z)}$ and $(\zeta_v^{(z)})'$ is negligibly small when compared with the experimental errors included in the absolute values of ζ_v. Thus, Eq. 34′ is used in the present investigation instead of Eq. 34, in which $(\zeta_v^{(z)})'$ is simply expressed as ζ_v.

Appendix III

Experimental methods for obtaining the correction terms of the rotational constants (α_i and β_i of Eq. 26) will be briefly discussed here. Table XXI includes the α_i's and β_i's hitherto observed. The superscripts I, M and O designate the experimental methods used (I: infrared, M: microwave, O: infrared overtone), while a)—e) indicate the authors.

An analysis of the microwave spectra gives extremely precise values of B_0 and, in some cases, B_v. However, the application of this method is limited to the "β_i" of lower vibrational frequencies, about 2000 cm^{-1} at most.

An analysis of the fine structures of the infrared and Raman spectra also gives the rotational constants, but such an analysis is usually restricted by the low resolving power of the instrument. Accurate values of α_i or β_i can be obtained by this method only if the individual rotational lines are well resolved.

For non-degenerate vibrational modes, β_i is obtained from a separation of resolved P- and R-branch lines ($\varDelta K=0$, $\varDelta J=\pm 1$), and α_i, from the K-dependence of center Q-branch lines ($\varDelta K$, $\varDelta J=0$).

For degenerate vibrations, the values of α_i are obtained from the K-dependence of ${}^{R}Q_K$ and ${}^{P}Q_K$ separations ($\varDelta J=0$, $\varDelta K=\pm 1$). The β_i's of the E-type might be obtained if the ${}^{R}P_K$, ${}^{R}R_K$, ${}^{P}P_K$ and ${}^{P}R_K$ lines are resolved. This is the case for the high-resolution studies of NH_3, ND_3, etc. However, in most cases of the E-type bands of methyl halides, these lines are weak and unresolved, making a smooth background for the prominent ${}^{R}Q_K$ and ${}^{P}Q_K$ lines. Recently, Brown and Edwards[28] observed these lines for some of the combination bands of CH_3Br and CH_3I. The resultant values of β are, however, not included in Table XXI because these values can not be reduced to those of the individual fundamental modes.

Overtone bands of a degenerate mode are sometimes useful for determining the β_i because an overtone band of E-type fundamentals consists of an A- and an E-type band, and the resolved A-type band gives the value $2\beta_i$. The values in Table XXI with the "O" superscripts and referred to as "overtone" in the footnote are one half of the $\beta_{2\nu_i}$ values.

When the individual lines are not resolved when their contours are observed (e. g., the Q branch of an A-type band, the ${}^{R}Q_K$ or ${}^{P}Q_K$ peaks of an E-type band, etc.), precise values of α_i or β_i are not obtained, as has been discussed in Appendix I. The sign of α_i or β_i is, however, known from the shape of the peaks; that is, α_i or β_i take a negative sign when the slope is steeper on the lower frequency side of the peak, and a positive sign in the opposite case. The terms in Table XXI with a + or − sign alone indicate that only the signs of α_i or β_i were determined in this way by the present investigation. The accuracy of the α_i and β_i values depends partly on the precision of the measurement. Another source of error lies, however, in the theoretical treatment; that is, apparent values of the rotational constants can not, in some cases, be expressed by such ordinary equations as are given in Eq. 26.

Two such cases are the rotational higher-order anharmonicity and the resonance through an accidental degeneracy of vibrational modes. Practically, therefore, the β_{ν_i} of an E-type fundamental band is not always just one-half of the $\beta_{2\nu_i}$, while some of the observed α_i or β_i values might be perturbed ones (e. g., the α_5 of CH_3I). Preliminary work on the effect of rotational resonance on α_i, according to the formulation of Nielsen,[21] suggests that the perturbation is fairly large even if the two resonating bands are separated by more than 50 cm^{-1} from each other. Similar situations have been recognized in microwave spectra.

---

[24] I. A. Kraitchman and B. P. Dailey, *J. Chem. Phys.*, **22**, 1477 (1954).

[25] T. Oka, private communication.

[26] J. Pickworth and H. W. Thompson, *Trans. Faraday Soc.*, **50**, 218 (1954).

[27] T. A. Wiggins, E. D. Shull and D. H. Rank, *J. Opt. Soc. Am.*, **43**, 157 (1953); *J. Chem. Phys.*, **21**, 1368 (1953).

[28] R. G. Brown and T. H. Edwards, ibid., **37**, 1029 (1962); ibid., **37**, 1035 (1962).